Supplementary data

1. Statistical responses from experimental design of ethanol injection method

Analysis of variance (ANOVA) was used to verify the statistical significance of the effect of the factors in the polydispersity and size responses (Table S.1). The result of the Fisher F-test was greater than the listed value for a 75% confidence level for the polydispersity and the size of liposomes; therefore, all factors significantly influenced the resulting particle size and polydispersity (Table S.1). However, the correlation coefficient (R^2) was 0.62 for liposome size in terms of the Z-average and 0.47 for liposome polydispersity, which indicated that the obtained mathematical model cannot be used to reach the optimum processing conditions.

Table S.1 - Analysis of variance and regression analyses for the response of the 23 central composite design.

Source of variation	Sum of square		Degrees of freedom		Mean square		*F*-test	
	Particle size*	PdI**	Particle size	PdI	Particle size	PdI	Particle size	PdI
Regression	890,574	0.304	6	4	148,429.0	0.076	2.69[a]	2.71[b]
Residual	551,325	0.338	10	12	55,132.5	0.028		
Lack of Fit	551,272	0.336	8	10	68,909.0	0.034		
Pure Error	53	0.002	2	2	26.5	0.001		
Total	1,441,899	0.642	16	16				

2. **Particle size is presented in terms of Z-average.*
3. ***PdI: abbreviation of polydispersity.*
4. *Regression coefficient: Particle size $R^2 = 0.62$; PdI $R^2 = 0.47$*
5. [a] $F_{6;\,10;\,0.25} = 1.58$
6. [b] $F_{4;\,12;\,0.25} = 1.55$

The response surfaces and contour plots (Figure S.1A, B and C) were chosen among the possible combinations to visualise the simultaneous effects of stirring rate, lipid concentration and injection flow on the Z-average of the obtained cationic liposomes.

A

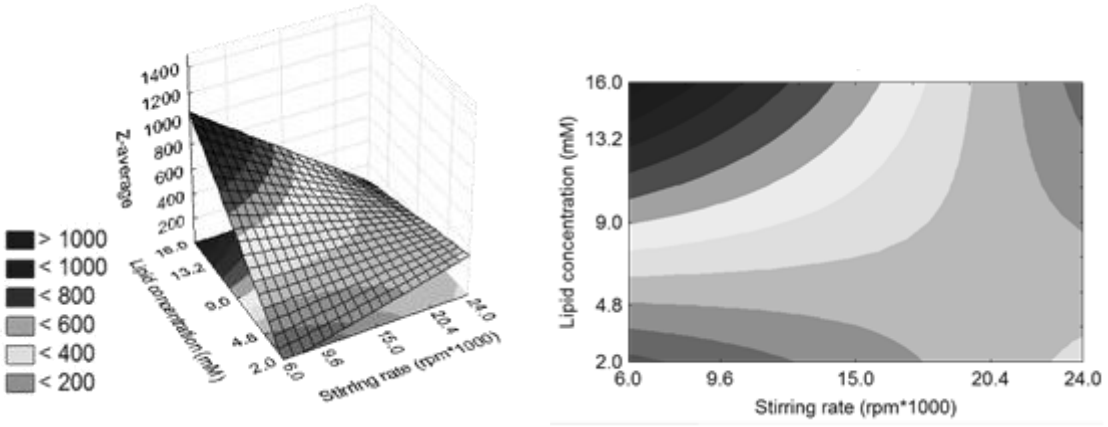

B

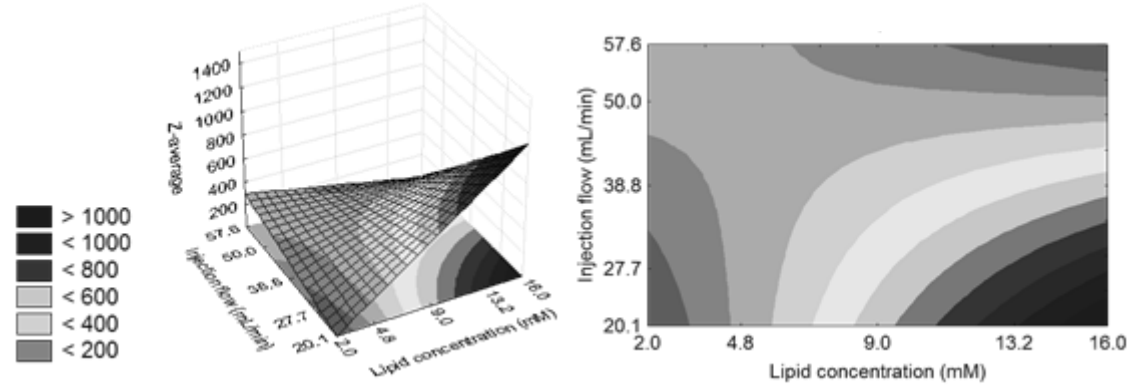

C

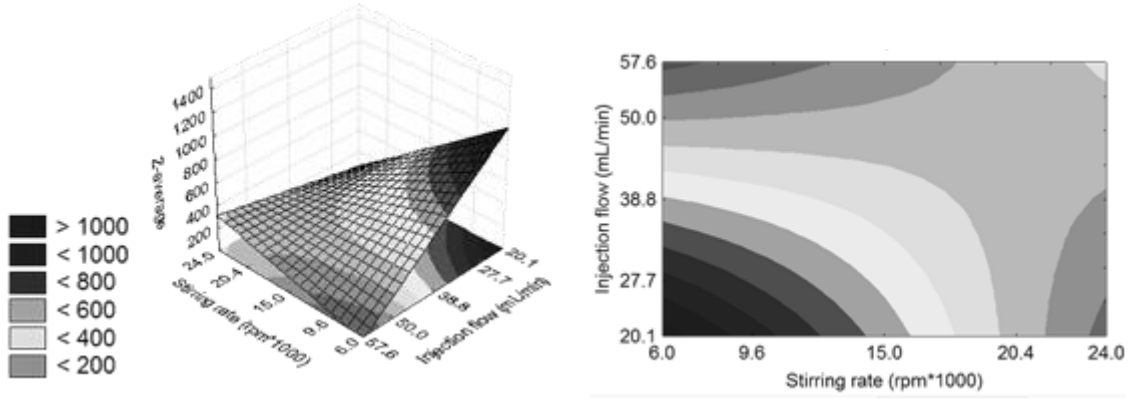

Figure S.1 – Response surface and contour curve for the Z-average as a function of (A) the stirring rate versus the lipid concentration, (B) the lipid concentration versus the injection flow and (C) the stirring rate versus the injection flow.

The size of liposomes decreases with a low final concentration and low stirring rate or with a high lipid concentration and a high stirring rate (Figure S.1A). The Z-average is not so affected by injection flow when the final lipid concentration is low; however, if the final lipid concentration is high, the injection

flow must also be high to decrease the size (Figure S.1B). Similarly, with a slow stirring rate and a fast injection flow or with a high stirring rate and a low injection flow, the size of cationic liposomes decreases (Figure S.1C).

The simultaneous effects of the stirring rate, the lipid concentration and the injection flow on the polydispersity of cationic liposomes are shown by the response surfaces and contour plots (Figure S.2A, B and C).

A

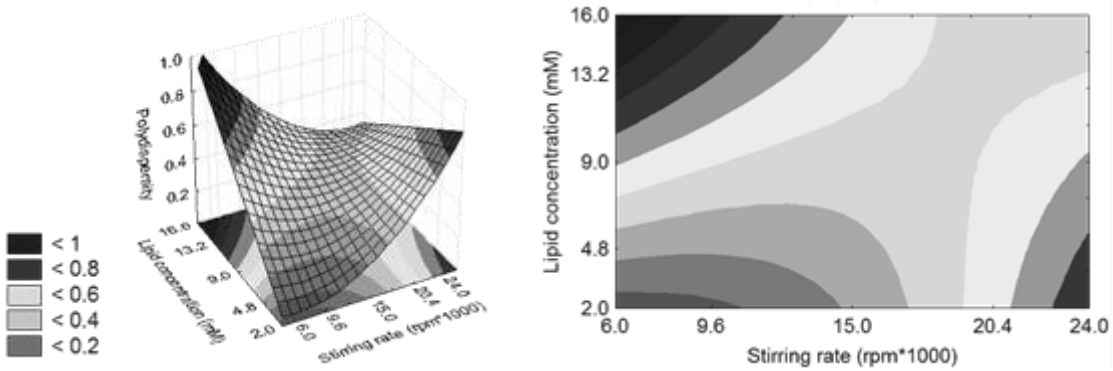

B

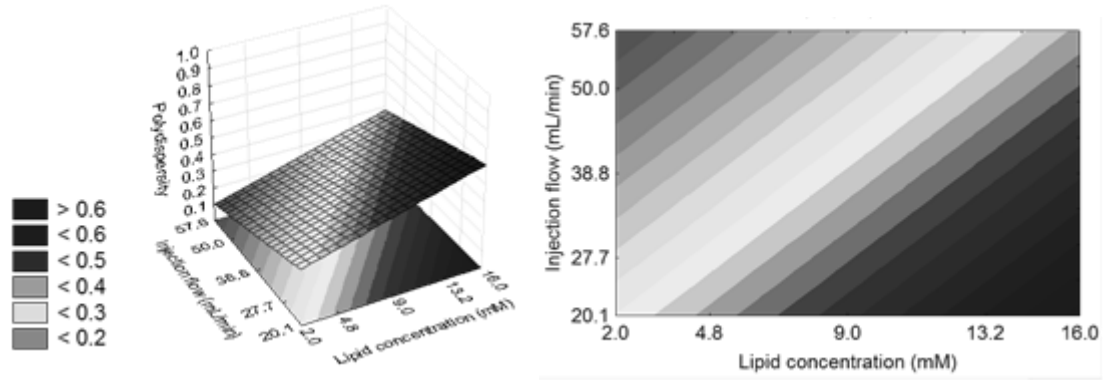

C

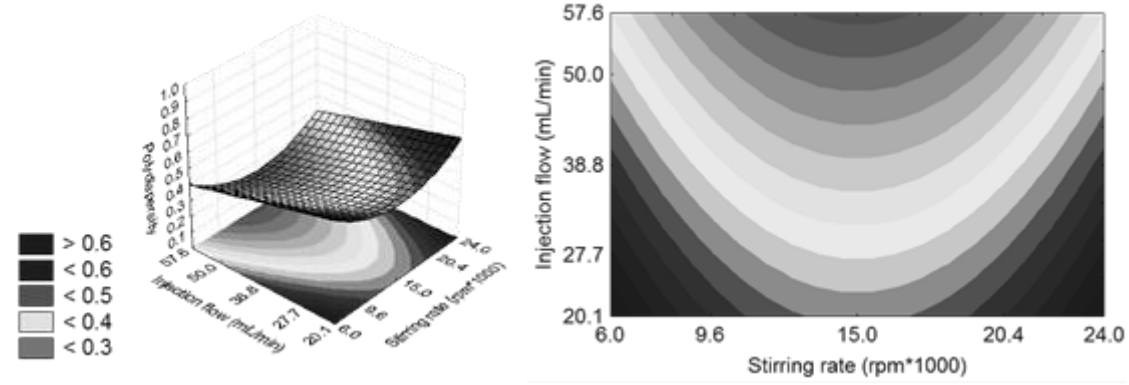

Figure S.2 – Response surface and contour curve for polydispersity as a function (A) the stirring rate versus the lipid concentration, (B) the lipid concentration versus the injection flow and (C) the stirring rate versus the injection flow.

The polydispersity of the liposome populations decreases with a low final concentration and a low stirring rate or with a high lipid concentration and a high stirring rate (Figure S.2A). Likewise, when the final lipid concentration is low and the injection flow is high, polydispersity decreases (Figure S.2B). The polydispersity of cationic liposomes decreases with a slow stirring rate and a

fast injection flow or with a high stirring rate and a high injection flow (Figure S.2C).

2. Physico-chemical properties of the ~~SM-liposomes~~MFV in function of cycles passed in microfluidizer

~~ST-liposomes~~VEI produced under optimized conditions were submitted to high-pressure microfluidization, which resulted in ~~SM-liposomes~~MFV. Figure S.3 presented ~~SM-liposomes~~MFV physico-chemical properties in terms of their size (Z-average) and their polydispersity as functions of the number of cycles.

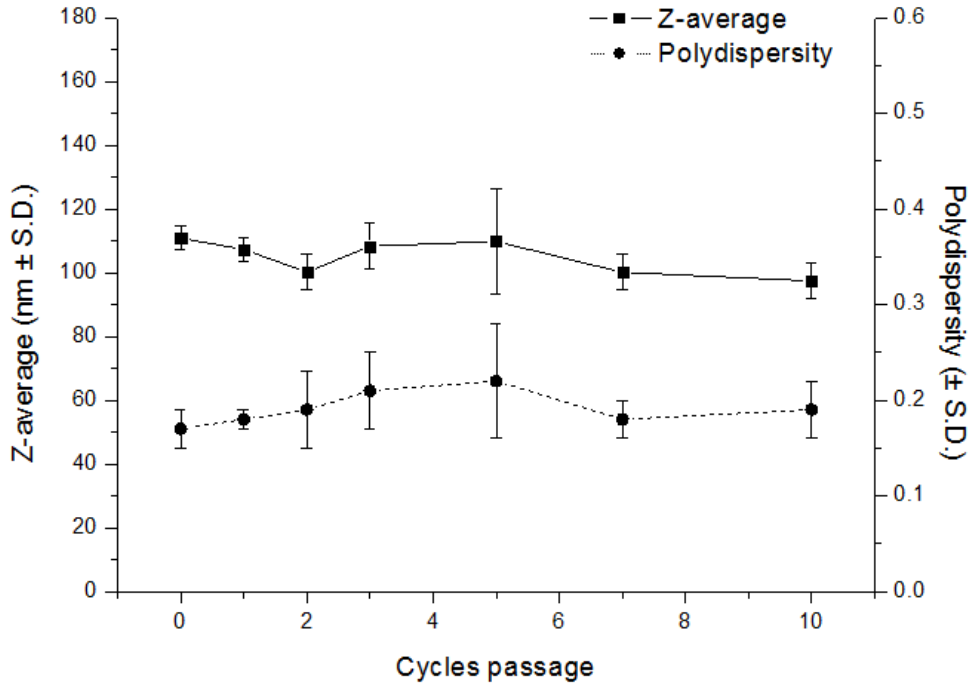

Figure S.3 – Z-average and polydispersity profiles of ~~SM-liposomes~~MFV obtained after microfluidization at 850 bar as functions of the number of cycles. The lines are for visual reference only.

3. Strategy of dendritic cells analysis

For phenotypic characterization and evaluation of the liposomes incorporation, we delimited gate with cell size and granularity compatible with the DCs, by analysis of the "side scatter" (SSC) - granularity (internal structure and complexity) and the "forward scatter" (FSC) - relative size of the cells (Figure S.4A). Considering the analyzed region bounded by the gate, cells were analyzed through the expression of the myeloid marker CD11c and the antigen presenting cells markers, HLA-DR. Furthermore, when we analyzed the

expression of co-stimulatory molecules within the population HLA-DR^{+}CD11c^{+}, called Gate R1 (Figure S.4B), we observed that cells also showed expression of CD86, antigen used to evaluate DCs activation. This procedure was performed for all samples, such as dendritic cells stimulated by TNF-α (positive control - mDC), or by ~~ST-liposomes~~VEI after optimization or by ~~SM-liposomes~~MFV after optimization.

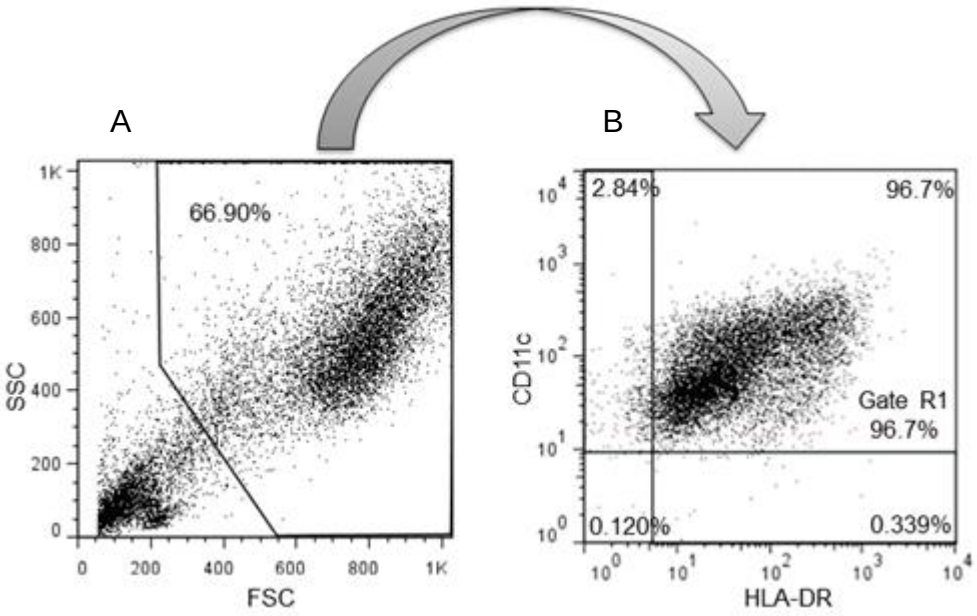

Figure S.4 – Strategy of dendritic cells analysis. (A) Dot Plot graph of SSC (side scatter) by FSC (forward scatter) to delimit DCs gate. (B) Graph of CD11c *versus* HLA-DR to delimit Gate R1, corresponding to cells double-positive.

4. Liposomes uptaken and CD86 expression on dendritic cells

In order to evaluate the phenotypic expression of DCs stimulated by liposomes, it was plotted graphics of CD86 versus liposomes' probe (Figure S.5) of dendritic cells stimulated by TNF-α (positive control - mDC) or by ~~ST-liposomes~~VEI or ~~SM-liposomes~~MFV. They showed that 49.1% of DCs had uptaken ~~ST-liposomes~~VEI and expressed CD86 (Figure S.5B), while 40.9% of DCs had uptaken ~~SM-liposomes~~MFV and expressed CD86 (Figure S.5C).

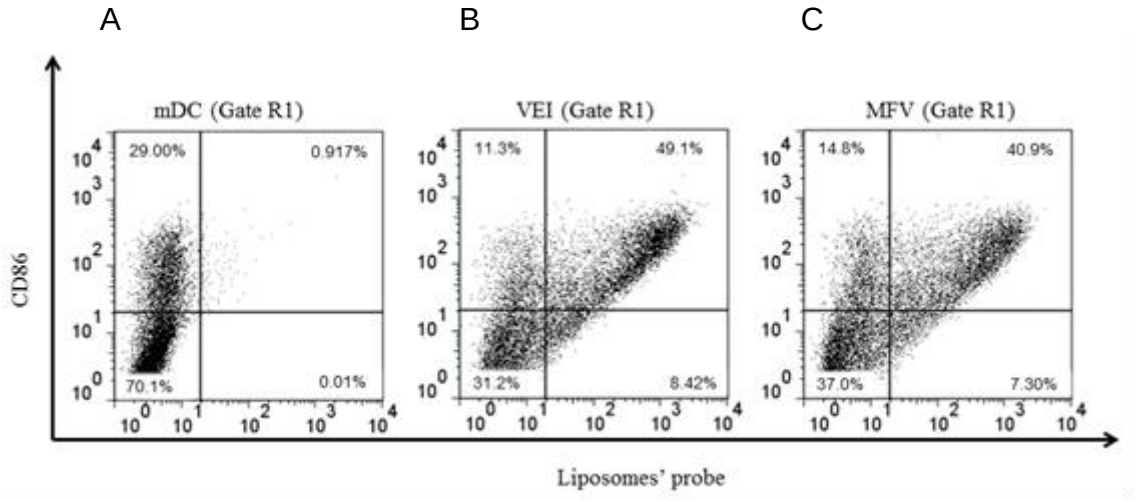

Figure S.5 – Expression of CD86 and liposomes' probe on dendritic cells stimulated by (A) TNF-α (positive control - mDC), (B) ~~ST-liposomes~~VEI after optimization (final lipid concentration of 2 mM, stirring rate of 11,000 rpm and injection flow of 44.4 mL/min) or (C) ~~SM-liposomes~~MFV after optimization (850 bar and 1 cycle passage).

5. Dendritic cell response to ethanol

Dendritic cell response to ethanol was studied to conclude if the amount of solvent present into liposomes added to stimulate DCs were not toxic for them. For this, we compared granularity (side scatter - SSC) and size (forward scatter - FSC) of iDC (immature dendritic cells) with those which received an amount of ethanol corresponding to the residue present in VEI and MFV before and after optimization (Figure S.6 A). As we can see in Figure S.6 A, there is no difference in iDC morphology due to ethanol addition. Moreover, we investigated a possible modification in DC behavior due to the presence of ethanol by a histogram of cell CD86 expression (Figure S.6 B). In this case either, there is no modification in DC behavior by the presence of 0.017% v/v ethanol (residue of ethanol present in liposome at 0.09 mM - lipid concentration per well). Thus, we can conclude that this amount of ethanol residue in VEI and MFV liposomes was non-toxic for DCs.

A B

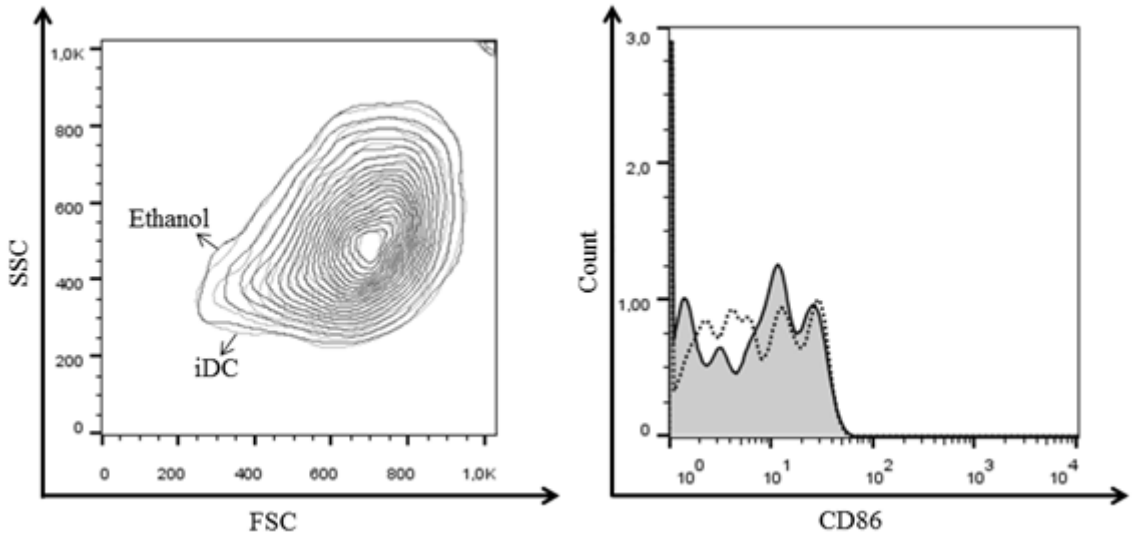

Figure S.6 – Dendritic cell response to ethanol residue from the liposomes. Contour plot SSC (side scatter) by FSC (forward scatter) (A) and CD86 histogram (B) of immature dendritic cells (iDC - color filled) or added 0.017% v/v of ethanol (dashed line), amount of solvent present in liposome at 0.09 mM (lipid concentration per well).